

Submitted to: 1987 Workshop on new develop-  
ments in particle acceleration techniques,  
Orsay, France 29 June - 4 July 1987

IL 40268

2  
CHOICE OF PARAMETERS FOR LINEAR COLLIDERS IN MULTI-BUNCH MODE\*

J. Claus  
(Brookhaven National Laboratory)

C  
BNL--40268

DE87 013648

2  
Abstract

The energy efficiency of a linear collider in multi-bunch mode is calculated for the case that the bunches in each of the two interacting beams are identical in all interaction points, a configuration which can be realized by taking advantage of the beam-beam effect between beams of opposite electric charge. The maximization of the efficiency is discussed, the maximum appears to increase nearly linearly with beam brightness and accelerating gradient, and about quadratically with the length of the IR. The optimum operating frequency for the linacs increases also, while the pulse repetition rate and the beam current needed for fixed luminosity, decrease. The increasing brightness and the decreasing current needed for higher efficiency lead to smaller transverse spotsizes in the crossing points; this imposes tighter tolerances on the relative transverse coordinates of the two beam-axes. Pillbox or similar resonators, excited in the TM<sub>01</sub> mode, may be preferable to quadrupoles for transverse focusing, at the high frequencies and gradients that seem desirable, particularly in the final focus.

---

## 1. INTRODUCTION

Multibunch operation of linear colliders has been discussed before [1,2,3]. It occurs if each of the two interacting particle beam pulses is composed of several bunches, rather than of a single one, as is more usually considered. It offers some freedom in the choice of the operating frequency of the two linacs, which can be exploited to minimize the rf energy required for a specified luminosity and length of interaction region. This subject was treated in [2] under the assumption that the beam-beam interaction in the IR could be neglected, which is clearly not realistic. This work was extended, now keeping account of the beam-beam effect, for the case that the bunches in each beam are all identical to each other in all interaction points. It is found, as expected from SLAC's disruption and R.B. Palmer's Superdisruption studies [4], that the beam-beam effect is beneficial. It appears again, that the efficiency (luminosity per unit rf power) can be maximized by proper choice of the operating frequency. Both the efficiency and the optimum frequency increase with increasing beam brightness and increasing accelerating gradient, while the beam current and pulse repetition rate required for fixed luminosity, decrease. The relation between efficiency and brightness is very nearly proportional, as is that between efficiency and gradient, it is therefore important to push both. It is even more important to choose the pulse length, i.e. the length of the IR, as long as is acceptable to the experimenters because the relation between efficiency and it is nearly quadratic. These calculations will have to be revised if a substantial fraction of the spent rf energy is recovered, particularly if the efficiency is low.

DISTRIBUTION OF THIS DOCUMENT IS UNLIMITED

*mgp*

\*Work performed under the auspices of the U.S. Dept. of Energy

**MASTER**

## 2. INTERACTION AREA

### 2.1 Beam self fields and transverse focusing

Studies of the beam-beam effect in storage rings, and of the so-called beam disruption in the crossing point of the SLC, show that the net transverse force felt by the individual particles from the self fields of highly relativistic beams is non-negligible in the regions where the particle distributions of the two opposing beams overlap and very small elsewhere. In the simple case of two bunched beams which move with equal velocities in opposite directions along a common axis, the regions where bunches can overlap are stationary in space. In passing through an opposing bunch each particle is exposed to its fields for a time interval  $\Delta t = l_b/(2\beta c)$ , with  $l_b$  the length of the bunch and  $\beta c$  the particle velocity, thus the effective longitudinal extent of the bunch field is  $l_{\text{eff}} = 0.5 l_b$ . The location where the first particle of a bunch first encounters an opposing bunch is half a bunchlength downstream of where its last one does so. The selffield of the opposing bunch has electric and magnetic components, described by:

$$E_r(r) = \Lambda r / (4\pi\epsilon_0 \rho^2), \quad B_\theta(r) = \mu_0 \beta c \Lambda r / (2\pi \rho^2) \quad (2.1.1)$$

if the charge density distribution is transversely uniform and the bunch is long compared to its diameter. Here  $\Lambda$  is the lineal charge density [C/m] in the bunch and  $\rho$  the beam radius. A particle of charge  $e$  and velocity  $v_1 = \beta_1 c$  experiences in that field a force:

$$F_r = e(E_r - \beta_1 c B_\theta) = \frac{e\Lambda r}{2\pi\epsilon_0 \rho^2} (1 - \beta_1 \beta) = \frac{\mu_0 e c^2 \Lambda r}{2\pi \rho^2} (1 - \beta_1 \beta) \quad (2.1.2)$$

If  $\beta_1 = \beta = 1$ , i.e., if particle and bunch have about equal velocities in the same direction,  $F_r = 0$ , if their velocities have opposite directions  $\beta_1 = -\beta$ ,  $\beta = 1$  and

$$F_r \cong 2 \frac{\mu_0 e c^2 r}{2\pi \rho^2} \quad (2.1.3)$$

with  $i$  the instantaneous current in the bunch. The force is focusing, since it is proportional to  $r$ ; it is truly focusing if the charges of particle and bunch have opposite signs, making  $F_r$  negative, as occurs when, e.g., electron bunches interact with positron bunches.  $F_r$  changes  $r' = dr/dz$ , where  $z$  represents displacement along the axis, at a rate:

$$\frac{dr'}{dz} = \frac{1}{mc^2 \beta^2} F_r \cong \pm 2 \frac{\mu_0 e c}{\gamma^2 \epsilon_0} \frac{1-r}{2\pi \rho^2} \quad (2.1.4)$$

where the + sign applies if the interacting bunches have equal, and the - sign if they have opposite polarities;  $\gamma$  is the Lorentz factor. If the change in the test particle's  $r$  remains disregardably small while it travels through the opposing bunch, that bunch acts as a thin lens with an inverse focal length  $q$  given by:

$$q \cong \pm 2 \frac{\mu_0 c}{E_0} \frac{1}{2\pi\gamma\rho^2} \int i \cdot dz = \pm \frac{\mu_0 c}{E_0} \frac{1}{2\pi\gamma\rho^2} i \cdot \lambda \quad (2.1.5)$$

where  $i$  is the beam current averaged over a r.f. period and  $\lambda$  the r.f. wavelength (= distance between successive bunch centers).  $i \cdot \lambda$  is a measure for the charge in the bunch, as is  $\int i \cdot dz$ . The integration interval in this integral is the effective axial length of the bunch field, thus half a bunchlength  $l_b$ , as mentioned before. Therefore:  $2 \int i \cdot dz = i \cdot \lambda$ . The lens is centered on the beam axis, and the lens action deflects the opposing beams towards each other (beams of opposite polarities) or away from each other (equal polarities) if they do not travel along the same axis.

In real bunches the current distribution is never uniform, as assumed, though generally bell shaped. This makes  $F_r$  non-linear in  $r$ , however,  $F_r(r)$  remains an odd function of  $r$  if  $i(r)$  is even, as is likely. The implied circular cylindrical symmetry can not be taken for granted either. Any quadrupole focusing along the route from source to interaction area will tend to introduce a cartesian symmetry. We will disregard these considerations in this discussion.

It is convenient to express  $q$  in terms of the beam brightness  $B$ , defined as  $B = i/\epsilon^2$ , where  $\epsilon$  is the invariant emittance of the beam, and the local amplitude function  $\beta$ :

$$q = \pm \frac{\mu_0 c}{E_0} \frac{(Bi)^{1/2}}{2\pi\beta} \lambda \quad (2.1.6)$$

since  $\rho^2 = \epsilon\beta/\gamma$ . To prevent possible confusion due to conflicting uses of  $\beta$ , this symbol will no longer be used to represent  $v/c$ , but only for Twiss and Frank's amplitude function. For  $v/c$  we shall write:

$$v/c = (1-1/\gamma^2)^{1/2} \cong 1-1/(2\gamma^2) \cong 1 \text{ for } \gamma \gg 1 .$$

## 2.2. Trains of bunches

The interaction between trains of bunches is complex because the interaction between any particular

$$q = \pm \frac{\mu_0 c}{E_0} \frac{(Bi)^{1/2}}{2\pi\beta} \lambda \quad (2.1.6)$$

since  $\rho^2 = \epsilon\beta/\gamma$ . To prevent possible confusion due to conflicting uses of  $\beta$ , this symbol will no longer be used to represent  $v/c$ , but only for Twiss and Frank's amplitude function. For  $v/c$  we shall write:

$$v/c = (1 - 1/\gamma^2)^{1/2} \cong 1 - 1/(2\gamma^2) \cong 1 \text{ for } \gamma \gg 1 .$$

## 2.2. Trains of bunches

The interaction between trains of bunches is complex because the interaction between any particular bunchpair, e.g., the  $k^{\text{th}}$  one from the left and the  $l^{\text{th}}$  one from the right, is determined by the, generally different, histories of each. However, if the two beams have opposite polarities, it appears possible to make all bunches of each beam, identical to each other in all crossing points. In that case each beam forms a periodic focusing system for the opposing one. If that beam is properly matched to the focusing system, its bunches will all have the same radius in all of the crossing points, presenting equally spaced focusing lenses of equal strengths to the counter streaming ones. Achieving this requires only that each beam enter the interaction region with the proper initial conditions (and that the bunches of each beam carry equal charges). Applying standard linear optics one finds for the value of  $\beta$  in the midplanes of the lenses and for the phase advance per cell  $\Delta\Psi$  of such a periodic system with lens strength  $q$  and a distance  $l$  between successive lens centers in the thin lens approximation:

$$\beta = \frac{l}{\sqrt{lq(1 - 1/4 lq)}} , \quad \sin(1/2 \Delta\Psi) = 1/2\sqrt{lq} \quad (2.2.1)$$

Substitution of  $l = 1/2 \lambda$  and of expression (2.1.6) for  $q$  yields a pair of coupled equations for the matched  $\beta$ 's of the two beams:

2

$$\beta_1 = \frac{\lambda\beta_2}{\sqrt{\lambda a_2(2\beta_2 - 1/4 \lambda a_2)}} , \quad \beta_2 = \frac{\lambda\beta_1}{\sqrt{\lambda a_1(2\beta_1 - 1/4 \lambda a_1)}} \quad (2.2.2)$$

where the subscripts 1 and 2 refer to the two beams, and where

$$a_j = q_j \beta_j = \frac{\mu_0 c}{2\pi E_0} (i_j B_j)^{1/2} \lambda , \quad j = 1, 2 \quad (2.2.3)$$

Separation yields:

$$x_i^{3/2} - 1/4 a_j \sqrt{\lambda a_i} x_i + 1/4 \lambda a_i x_i^{1/2} - (\lambda^2/a_j)/\sqrt{\lambda a_i} = 0 \quad (2.2.4)$$

where  $x_i$  stands for:

$$x_i = 2\beta_i - 1/4 \lambda a_i$$

and where  $i = 1, j = 2$ , or  $i = 2, j = 1$ . Equations (2.2.4) have at least one real root for  $x_i$ , which has for both beams the simple form:

$$x = \lambda/a \quad (2.2.5)$$

if  $a_i = a_j = a$ ; this applies, e.g., when the two beams have equal brightnesses and currents, and yields for  $\beta$ :

$$\beta = 1/2 \lambda (1/a + 1/4 a) \quad (2.2.6)$$

I have found no convenient analytic solution for  $x_{1,2}$  if  $a_1 \neq a_2$ , but numerical experimentation suggests that the two beams can be matched to each other even so; I surmise that that is still true if they have two transverse axes of symmetry, instead of being circular cylindrical.

### 2.3 Luminosity

beams the simple form:

$$x = \lambda a \quad (2.2.5)$$

if  $a_1 = a_2 = a$ ; this applies, e.g., when the two beams have equal brightnesses and currents, and yields for  $\beta$ :

$$\beta = 1/2 \lambda (1/a + 1/a) \quad (2.2.6)$$

I have found no convenient analytic solution for  $x_{1,2}$  if  $a_1 \neq a_2$ , but numerical experimentation suggests that the two beams can be matched to each other even so; I surmise that that is still true if they have two transverse axes of symmetry, instead of being circular cylindrical.

### 2.3 Luminosity

The luminosity produced by the interactions between two trains of identical bunches that move in opposite directions along a common axis can now be estimated. We calculate first the time integrated luminosity (TIL,  $\mathcal{L} = \int L dt$ ) from two interacting bunches. The TIL from the two trains, each  $N$  bunches long, is  $N^2$  times that from a single bunch pair, since each bunch in each train interacts with all of the bunches in the other. If the process is repeated at a rate  $f$  per unit time the time average luminosity becomes:  $L = fN^2\mathcal{L}$ .

The TIL from a single bunch pair may be described by:

$$\mathcal{L} = \frac{n_b^2}{4\pi\sigma^2} = \frac{\gamma n_b^2}{4\pi\epsilon\beta} = \frac{\gamma(c\lambda e)^2 Bi}{4\pi\beta} \quad (2.3.1)$$

where  $n_b$  is the number of particles per bunch and  $s$  the rms bunch radius under the assumption that the transverse distribution is Gaussian. Substitution of (2.2.6) and (2.2.3) yields an expression for the integrated luminosity from a single pulse, which, for the case of equal brightnesses and currents, may be written in the form:

$$\mathcal{E} = (L_B + \lambda)^2 \frac{\gamma}{\pi} \left(\frac{c}{v}\right)^2 \left(\frac{H_0 c}{4\pi I_0}\right) \frac{(tB)^{3/2}}{1 + \left(\frac{H_0 c}{4\pi I_0}\right)^2 tB \lambda^2} \quad (2.3.2)$$

Here is  $L_B = (N-1)\lambda$  the distance between the centers of the first and the last bunch in a beam pulse, thus the length of the inter-action region if both beams have the same number of bunches  $N$ . This substitution is only approximately valid because the expression for the luminosity assumes a Gaussian distribution in each bunch, while the expression for  $\beta$  assumes a transversely uniform one. I will disregard the difference as being of little consequence for the present purpose.

### 3. LINAC AND BEAM CURRENT

In a previous paper [2] an expression was derived for the energy that the power source must supply to a linac for the acceleration of a beam pulse with specified characteristics. There is also an expression for the maximum beam current. These formulae are valid for linacs that are composed of resonant cells that are coupled individually to the rf power source. They may be said to be supplied in parallel. Such linacs deviate from the conventional ones, which may be regarded as disk loaded wave guides or, alternatively, as strings of resonant cells in which the rf power flows from one cell to the next one, supplying them in series. Linacs of the proposed type may have some advantages at the very short wavelengths that seem desirable for reasons of energy efficiency and their principal characteristics are easily calculated. We repeat the relevant expressions for the convenience of the reader:

$$E_s = \frac{\gamma E_0}{0.8 F_{tr}} 1/2 i^2 R_0 \tau_B (1+x)^2 [1+a \ln(1+x)] \quad (3.1)$$

where:

$$x = \frac{0.8}{2iR_0} (1+R_0/R) = \frac{2\pi}{\bar{\alpha}} \frac{Z_c}{R_0} (1+R_0/R) \quad (3.1.1)$$

$$a = \tau/\tau_B \quad (3.1.2)$$

$$i = \frac{1}{4\pi F_{tr}} \frac{\bar{\alpha}}{Z_c} 0.8 \quad (3.1.3)$$

$$0.8 = g\lambda \mathcal{E} \quad (3.1.4)$$

$$Z_c = \frac{R}{Q} \left[ 1 - \left(\frac{1}{2Q}\right)^2 \left(1 + \frac{R}{R_0}\right)^2 \right]^{-1/2}$$



2

and where:

$E_s$  rf energy delivered by the source,

$i$  beam current

$\tau_B$  length of the beampulse in time, ( $\tau_B \cdot c = L_B$ )

$\bar{E}$  amplitude of the accelerating field

$\bar{U}_g$  gap voltage

$g$  gap length in terms of rf wavelengths  $\lambda$

$F_{tr}$  transit time factor

$R_o$  source impedance per cell

$R$  shunt resistance per cell

$Q$  Q factor per unloaded cell

$\tau$  time constant per cell ( $\omega_r \tau = 2Q/(1+R/R_o)$ )

$Z_c$  geometric factor, depends upon the relative distributions of the electric and magnetic fields in the cell, thus on the shape of the cell, but is largely independent of its resonant frequency, thus of its size ( $Z_c \cong \sqrt{L/C}$ ).

$\bar{\alpha}$  energy gain per bunch per cell as a fraction of the energy stored per cell.

#### 4. EFFICIENCY

Division of (2.3.1), which describes the time integrated luminosity per pulse by (3.1), which gives rf energy delivered by the rf source as needed by that pulse, yields the  $\eta$  per unit of energy and at the same

$\tau$  time constant per cell ( $\omega_r \tau = 2Q/(1+R/R_0)$ )

$Z_c$  geometric factor, depends upon the relative distributions of the electric and magnetic fields in the cell, thus on the shape of the cell, but is largely independent of its resonant frequency, thus of its size ( $Z_c \cong \sqrt{L/C}$ ).

$\bar{\alpha}$  energy gain per bunch per cell as a fraction of the energy stored per cell.

#### 4. EFFICIENCY

Division of (2.3.1), which describes the time integrated luminosity per pulse by (3.1), which gives rf energy delivered by the rf source as needed by that pulse, yields the TIL per unit rf energy and at the same time the luminosity (averaged over time) per unit (average) rf power. It may be written in the form:

$$\eta_L = \frac{L}{P_{\text{rfs}}} = \frac{\int L dt}{E_{\text{rfs}}} = \frac{8}{\mu_0 (ec)^2} \frac{a}{L_B} \left( \frac{x}{1+x} \right)^2 \frac{y \cdot (1+y)^2}{[1+b \cdot y \cdot \ln(1+x)] \cdot (1+a \cdot y^3)} \quad (4.1)$$

where:

$$x = \frac{2\pi}{\bar{\alpha}} \frac{Z_c}{R_0} (1 + R/R_0) \quad (4.1.1)$$

$$y = \lambda/L_B \quad (4.1.2)$$

$$a = \left( \frac{\mu_0 c}{4\pi E_0} \right)^2 \frac{\bar{\alpha} g \bar{E} B L_B^3}{4\pi F_{\text{tr}} Z_c} \quad (4.1.3)$$

$$b = 2\bar{\alpha}$$

(4.1.4)

and where the parameters  $y$ ,  $a$ , and  $b$  have been introduced for reasons of convenience. Inspection shows that  $\eta_L$  is proportional with  $a/L_B$ , and that it can be maximized by proper choice of  $x$  and  $y$ .

The opportunities for the maximization of  $a/L_B$  are somewhat limited. The field  $E$  in the cavities is restricted to no more than a few GV/m, depending on frequency and pulse length, by surface effects at the cavity walls (field emission and photo emission, due to synchrotron light, of electrons, thermal effects due to dissipation).

The beam brightness  $B$  is restricted by the source, and can be reduced seriously by transverse wakefields and by non-linearities in the transverse motion. As a measure of the density in four dimensional transverse phase space it is expected to depend less on the beam current than the emittance does. The value of  $g/F_{tr}$  determined by the design of the linac, leaves little choice:  $\pi/4.5 \leq g/F_{tr} \leq \pi/4$  for phase advances per cell between  $(2/3)\pi$  and  $\pi$ , and decreases quickly for smaller phase advances.

The cavity loading factor  $\bar{\alpha}$  is limited to perhaps  $\bar{\alpha} \leq 0.05$  (SLAC number) by considerations of beam stability (wake fields) and momentum spread (constraint imposed by the users), a limit that may well depend on bunch length  $\lambda$ , becoming smaller for shorter bunches.

The length of the interaction region  $L_B$  should be chosen as long as is still acceptable to the users, who should be aware that its choice affects the efficiency quadratically: double the source length gives four times the luminosity for the same momentum if the efficiency is low, as is likely.

The efficiency can be maximized for given values of  $a/L_B$  by proper choice of the source impedance  $R_0$  and the wavelength  $\lambda$ , in view of (4.1.1) and (4.1.2). Since analytic expressions for the maximized efficiency and the values for  $R_0$  and  $\lambda$  at the maximum appeared to be inconvenient we calculated a number of examples numerically. Our results are shown in Figs. (4.1-4.7). The beam brightness  $B$  was chosen as independent parameter in all cases because we are least certain about what its value might be. That is also the reason for the large interval of variation chosen. It contains the brightness that is expected for the SLAC linear collider ( $B = 3 \cdot 10^{10} \text{ A/(rad-m)}^2$ ). Although continuous curves are shown, only the points associated with  $B$ 's which yield  $\lambda = L_B/(n_b - 1)$ , with  $n_b$  the number of bunches per pulse, are valid, because the interaction region is an integer number of wavelengths long.

Figures (4.1-4.3) represent results obtained for the parameter set  $E = 1 \text{ GV/m}$ ,  $L_B = 1 \text{ cm}$ ,  $\bar{\alpha} = 0.05$ . Most of them are bounded on the left side by the consideration that  $\lambda \leq L_B$ ; this condition is violated if  $B$  is chosen too small. The crucial curve in these graphs is the one for  $1/\eta_L$  (Fig 4.1), which describes the rf power required per unit luminosity. It behaves approximately as  $1/\eta_L = 2.0 \cdot 10^{-20} B^{-0.78}$ , and shows, e.g., that a facility with a luminosity of  $L = 10^{35} \text{ cm}^{-2} \text{ sec}^{-1} = 10^{-39} \text{ m}^{-2} \text{ sec}^{-1}$ , would require a rf power of 50GW if the beam brightnesses are  $B = 10^{11} \text{ A/(rad-m)}^2$ , while only 27MW would be needed if  $B = 10^{15} \text{ A/(rad-m)}^2$  could be achieved.

locations, e.g., in the interaction area. There, the distance between the two beams must be small compared to the smallest beam radius, e.g.,  $0.1 \rho$ , and their axes may not deviate from parallelness by more than a small fraction of the half angular spread in each beam, e.g.,  $0.1 \rho'$ . The coordinates of the beam axes will vary with time in response to, e.g., temporal displacements of the source and of the focusing elements. Servo systems, that redirect the beams in response to measured deviations from target values, can be introduced to minimize the magnitude of this random motion of the beam axes, but cannot eliminate it because of noise, timedelays and limited bandwidths in the loops, and the position and direction of each beam axis will still change from pulse to pulse. The magnitude of this residual motion must be kept within acceptable bounds. Figure 4.2 shows that, at  $\gamma = 10^7$ , the beam has a diameter of a half  $\mu\text{m}$  or so in the crossing points, even at the lowest brightness and also that it decreases with brightness as  $B^{-0.5}$ , implying the need of a relative position control of better than 25nm to 25pm.

We discuss the focusing conditions in linacs and interaction region separately because they are so very different. The linacs represent systems that stretch over several km's each, and the diameter of the beam is not of much consequence, provided that it fits everywhere inside the available effective aperture. They are the sources that supply the interaction region with beams and must meet the requirement that the deviations of the coordinates of each beam axis remain small compared to the beam emittance in  $xx'yy'$ -space at the interfaces with the interaction region. If this region can be kept relatively small in extent, it may be possible to decouple it from the outside world as a unit. The final focusing systems, which convert the incident beams to the ones wanted in the interaction region, would be part of that unit.

### 5.1. Linac cells as focusing elements

The transverse motion is usually controlled by means of quadrupoles. The high fields and short wavelengths that characterize the linacs under discussion suggest the use of similar structures as focusing elements. In the TM01 mode there exists in each linac cell a toroidal transverse magnetic field, that is independent of the axial position  $z$  and that behaves transversely approximately as

$$B_{\theta}(r) = i \frac{k}{\omega} E J_1(kr) \quad (5.1.1)$$

to decouple it from the outside world as a unit. The final focusing systems, which convert the incident beams to the ones wanted in the interaction region, would be part of that unit.

### 5.1. Linac cells as focusing elements

The transverse motion is usually controlled by means of quadrupoles. The high fields and short wavelengths that characterize the linacs under discussion suggest the use of similar structures as focusing elements. In the TM<sub>01</sub> mode there exists in each linac cell a toroidal transverse magnetic field, that is independent of the axial position  $z$  and that behaves transversely approximately as

$$B_{\theta}(r) = i \frac{k}{\omega} E J_1(kr) \quad (5.1.1)$$

$$\partial B_{\theta} / \partial r = i \frac{k^2}{2\omega} E [J_0(kr) - J_2(kr)] = i \frac{\pi}{c\lambda} E J_0(kr) \approx \quad (5.1.2)$$

$$\approx i \frac{\pi}{c\lambda} E, \text{ provided that } kr = 2\pi r/\lambda \ll 1$$

in the case of a cylindrical pillbox resonator and as

$$B_x(y) = -i \frac{k}{\omega} E \cos(kx) \sin(ky), \quad B_y(x) = i \frac{k}{\omega} E \sin(kx) \cos(ky) \quad (5.1.3)$$

$$\partial B_x / \partial y = -i \frac{k^2}{\omega} E \cos(kx) \cos(ky), \quad \partial B_y / \partial x = i \frac{k^2}{\omega} E \cos(kx) \cos(ky) \quad (5.1.4)$$

$$\approx -i \frac{\pi}{c\lambda} E, \quad \approx i \frac{\pi}{c\lambda} E,$$

2

beam, would demand  $f = 10^{39}/(10^7 \cdot 4 \cdot 10^{26}) = 250$  kHz at  $B = 10^{11}$  A/(rad-m)<sup>2</sup>, while  $f = 20$  kHz would be adequate at  $B = 10^{15}$  A/(rad-m)<sup>2</sup>. We note that SLAC's SLC is expected to operate at  $B = 2.5 \cdot 10^{10}$  A/(rad-m)<sup>2</sup> and  $f = 180$  Hz.

$P_s$  (MW) represents the rf power during the pulse.

$\tau_s$  (psec) is the pulse length of the rf source, as seen from a single cell, while  $\tau_B$  (psec) is the length of the beam pulse,  $\tau_B = L_B/c$ ;  $\tau_s - \tau_B$  is the filling time for that cell. At least one power source must be active as long as the pulse is still in the linac, thus the rf energy delivered per pulse is at least  $E_s = P_s E_f / (E \cdot F_{tr})$ , where  $E_f$  is the final energy in eV.

$\lambda \leq L_B$  (cm) is the wavelength of the rf.

Figure 4.2 gives the behaviour of the beam current  $I_b$ , averaged over the pulse, and that of its invariant emittance  $\epsilon$ . Also shown are the beam radius  $\sigma\sqrt{\gamma}$  in the crossing points and the value of  $\beta$  that must be produced by the final focusing system in order to establish the matched condition on which this discussion is based.

Figure 4.3 gives the betatron phase advance  $\Delta\psi$  between two successive crossing points and  $\eta_{rf}$ , a parameter that indicates what fraction of the incident rf energy ends up in the beam (the remainder,  $1 - \eta_{rf}$ , is either reflected back towards the power source or dissipated). Note that this figure is linear in the  $\Delta\psi$  and  $\eta_{rf}$  axes.

Figure 4.4 shows the behaviour of  $1/\eta_L$  as a function of  $\lambda$  for fixed  $B$ ,  $L_B$ ,  $\bar{\alpha}$  and  $\bar{E}$ .  $\lambda$  is chosen and the source impedance is adjusted for a minimum in  $1/\eta_L$ . It may be seen that deviations of  $\lambda$  within a factor of two from the optimum value causes deterioration of  $1/\eta_L$  by factors larger than three. It is thus important that  $\lambda$  be chosen correctly, if at all possible. However, the shape of this curve may depend on the choice of the parameters  $B$ ,  $L_B$ ,  $\bar{\alpha}$  and  $\bar{E}$ , and the sensitivity to deviations of  $\lambda$  from its optimum may be different. The parameters for the curve shown are:

parameter that indicates what fraction of the incident energy ends up in the beam (the remainder,  $1-\eta_{\text{eff}}$ , is either reflected back towards the power source or dissipated). Note that this figure is linear in the  $\Delta\psi$  and  $\eta_{\text{eff}}$  axes.

Figure 4.4 shows the behaviour of  $1/\eta_L$  as a function of  $\lambda$  for fixed  $B$ ,  $L_B$ ,  $\bar{\alpha}$  and  $\bar{E}$ .  $\lambda$  is chosen and the source impedance is adjusted for a minimum in  $1/\eta_L$ . It may be seen that deviations of  $\lambda$  within a factor of two from the optimum value causes deterioration of  $1/\eta_L$  by factors larger than three. It is thus important that  $\lambda$  be chosen correctly, if at all possible. However, the shape of this curve may depend on the choice of the parameters  $B$ ,  $L_B$ ,  $\bar{\alpha}$  and  $\bar{E}$ , and the sensitivity to deviations of  $\lambda$  from its optimum may be different. The parameters for the curve shown are:

$$B = 10^{16} \text{A}/(\text{rad-m})^2, \quad L_B = 1\text{cm}, \quad \bar{\alpha} = 0.05, \quad \bar{E} = 1\text{GV/m}.$$

Figures (4.5-4.7) show how  $1/\eta_L$ ,  $1/\gamma Ldt$ ,  $P_s$ ,  $\tau_s$  and  $\lambda$  respond to changes in the choice of parameters. They only illustrate what can be seen from (4.1): reductions in  $\bar{\alpha}$ ,  $\bar{E}$  and  $L_B$  all lead to increases in the power needed for a specified luminosity. In particular: a reduction of  $L_B$ , the length of the interaction region from 1cm to 1mm is only possible (in this mode of operation) if a brightness of at least  $1 \cdot 10^{13} \text{A}/(\text{rad-m})^2$  is available; for that brightness  $1/\eta_L = 2.7 \cdot 10^{-29} \text{Wm}^2 \text{sec}$ , while it is  $1/\eta_L = 1.1 \cdot 10^{-30} \text{Wm}^2 \text{sec}$  for the same brightness and  $L_B = 1\text{cm}$ , a factor 25 better. Note that the optimum wavelength increases a little, from  $\lambda = 0.72\text{mm}$  for  $L_B = 1\text{cm}$  to  $\lambda = 1\text{mm}$  for  $L_B = 1\text{mm}$ .

## 5. TRANSVERSE MOTION

The previous discussion is based on the assumption that the two participating beams move in opposite directions along a common axis. In practice, each beam starts from a source and is guided towards the interaction region by a transverse focusing system which is incorporated in each linac and in each beam transport system. Steering elements are provided to place and direct the beam as desired at particular

provided that  $kx = \pi\sqrt{2} x/\lambda, \ll 1, ky = \pi\sqrt{2} y/\lambda, \ll 1$ , in the case of a pillbox resonator of square cross-section. In these expressions  $E$  is, as before, the electric field on the axis, harmonic time dependence with frequency  $\omega/2\pi$ , free space wavelength  $\lambda$ , and operation at the resonant frequency is understood,  $i = \sqrt{-1}$ .  $E$  and  $B_{0,x,y}$  differ in phase by  $\pi/2$  rad, thus the principal difference between accelerating cells and focusing cells is the phase with which they are run relative to the beam bunches. The average focusing gradient can be related to the instantaneous ones given, by transit time factors  $F_{tr}$ ,  $2/\pi \leq F_{tr} < 1$ , which account for the changes in the cell fields that occur during the time spent by a bunch in a cavity of finite length, and for the field distortions that exist in the vicinity of the holes for beam passage in the cavity side walls. Doing so we obtain for the focusing gradient  $B' = \partial B/\partial r$ , where  $r$  stands for  $r = (x^2 + y^2)^{1/2}$ :

$$B' = \frac{\pi}{c\lambda} E F_{tr} \quad (5.1.5)$$

Approximating  $F_{tr}$  with  $F_{tr} = \sin(\pi g)/(\pi g)$ , with  $g$  defined as before, one finds with  $E = 10^6$  V/m,  $\lambda = 0.1$  mm,  $g = 0.5$ :  $B' = 6.7 \cdot 10^4$  T/m, equivalent to the gradient in a quadrupole with a poletip field of 1 T and a throat circle radius of 16  $\mu$ m. One advantage of a linac section as focusing element is, that it focuses (or defocuses, depending on the phase with which it is driven) equally in both transverse directions, while a quadrupole focuses in one, but defocuses in the other. This makes the linac section more effective than combinations of quadrupoles with the same gradient for some application, e.g. the final focus.

## 5.2. Choice of parameters

A discussion of some of the effects of misalignments of focusing elements in a linac is given in appendix A. It appears that the tolerances on the alignment decrease with increasing beam brightness, and that they are maximized by using all of the available aperture everywhere. That aperture is a fraction of the wavelength, 0.25 $\lambda$ -0.2 $\lambda$  or so, depending on the structure; the (2.5 $\sigma$ ) diameter of the beam can only be a fraction of that, perhaps 1/3, thus the effective beam radius  $\rho$  can be no more than a few percent of the wavelength:  $\rho \leq 0.04\lambda$ . One may see from Figs. 4.1 and 4.2, that the behaviour of  $\lambda$  and of  $\epsilon$  as functions of  $B$  may be crudely approximated by:

$$\lambda = 26.02B^{-0.34}, \quad \epsilon = 638.7B^{-0.67} \quad (5.2.1)$$

for  $L_B = 1$  cm,  $\bar{\alpha} = 0.05$ ,  $\bar{E} = 1$  GV/m. It follows, that the  $\beta$  wanted at the exit of the linac is practically independent of  $B$  and proportional to  $\gamma$ :

$$\beta = \gamma^2/\epsilon = 0.0004\gamma, \quad \text{if } \rho = 0.02\lambda \quad (5.2.2)$$

so that  $\beta = 4000$  m at  $\gamma = 10^7$ . This  $\beta$  must be matched to the  $\beta_{mn}$  in the interaction region, 1/4 $\lambda$  upstream of the first crossing point, which behaves approximately as:

$$\beta_{mn} = 6.681B^{-0.33} \quad (5.2.3)$$

as shown by Fig. 4.3. The final foci must therefore have transfer functions with linear (de)magnification factors of  $(\beta/\beta_{mn})^{1/2} = 24B^{1/6}$ , e.g., about 940 at  $B = 10^{10}$  A/(rad-m)<sup>2</sup> and about 8400 at  $B = 10^{16}$  A/(rad-m)<sup>2</sup>. This is achieved if they have transfer matrices of the form



$$|M|_{\text{linac} \rightarrow \text{IR}} = \begin{pmatrix} (\beta_{\text{min}}/\beta)^{1/2} & 0 \\ 0 & (\beta/\beta_{\text{min}})^{1/2} \end{pmatrix} = \begin{pmatrix} 1/(24B^{1/6}) & 0 \\ 0 & 24B^{1/6} \end{pmatrix} \quad (5.2.4)$$

$$|M|_{\text{linac} \rightarrow \text{IR}} = \begin{pmatrix} 0 & (\beta_{\text{min}}/\beta)^{1/2} \\ -(\beta/\beta_{\text{min}})^{1/2} & 0 \end{pmatrix} = \begin{pmatrix} 0 & 0.0027\gamma B^{-0.33} \\ -1/(0.0027B^{-0.33}) & 0 \end{pmatrix} \quad (5.2.5)$$

Numerically we obtain for  $\gamma = 10^7$  and  $B = 10^{10} \text{ A/(rad-m)}^2$ :

$$|M|_{\text{linac} \rightarrow \text{IR}} = \begin{pmatrix} 1/967 & 0 \\ 0 & 967 \end{pmatrix} \text{ or } |M|_{\text{linac} \rightarrow \text{IR}} = \begin{pmatrix} 0 & 3.30 \\ -1/3.30 & 0 \end{pmatrix}$$

and for  $\gamma = 10^7$  and  $B = 10^{16} \text{ A/(rad-m)}^2$ :

$$|M|_{\text{linac} \rightarrow \text{IR}} = \begin{pmatrix} 1/8600 & 0 \\ 0 & 8600 \end{pmatrix} \text{ or } |M|_{\text{linac} \rightarrow \text{IR}} = \begin{pmatrix} 0 & 0.33 \\ -1/0.33 & 0 \end{pmatrix}$$

The anti diagonal matrix can be realized with a single triplet of thick quadrupoles and also with a linac section. The magnitude of the  $m_{12}$  element is restricted by the available focusing gradient, which limits the achievable demagnification. Nearly arbitrarily large demagnification factors can be obtained from more complex systems. They might have a diagonal transfer matrix and their lengths would increase with decreasing available gradient. This would affect their sensitivity for misalignments unfavourably; it follows that high gradients are desirable.

## REFERENCES

- [1] B. W. Montague, CLIC Notes 11, 17, CERN, January, March 1986
- [2] J. Claus, "Energy Efficiency and Choice of Parameters for Linear Colliders," paper presented at the "Seminar on New Techniques for Future Accelerators," Erice, Sicily, Italy, May 11-17, 1986, Proceedings to be published in the "Ettore Majorana International Science Series," by Plenum Press, New York, September 1987
- [3] B. W. Montague, "Self-focusing multi bunch crossings," unpublished paper presented at the Conference on "Critical Issues in the Development of New Linear Colliders," Madison, Wisconsin, August 27-29, 1986
- [4] R. B. Palmer, SLAC-PUB-3688, May 1985

2

Appendix A

MISALIGNMENTS IN LINAC

We consider some of the consequences of misalignments of the quadrupoles of a linac. We treat the quadrupoles as thin lenses, and assume that there is no coupling between the two orthogonal components ("horizontal" and "vertical" or "x" and "y") of the transverse motion. The quadrupoles are disposed and excited to form a periodic focusing system, however, the constants of that system may change gradually, i.e., adiabatically, along the length of the linac. The half cell length  $l$ , the inverse focal length  $q$  of the quadrupoles, the betatron phase advance per cell  $\Delta\psi$  and the amplitude functions  $\beta_f$  and  $\beta_d$  in the focusing and defocusing quadrupoles of a conventional FODO lattice are related according to:

$$\sin(\Delta\psi/2) = \text{sn} = lq/2 \tag{A.1a}$$

$$\beta_f = \frac{l}{\text{sn}} \left( \frac{1 + \text{sn}}{1 - \text{sn}} \right)^{1/2}, \quad \beta_d = \frac{l}{\text{sn}} \left( \frac{1 - \text{sn}}{1 + \text{sn}} \right)^{1/2} \tag{A.1b}$$

The displacement of a quadrupole with inverse focal length  $q$  over a distance  $x$  from its reference position is equivalent to the introduction of a dipole moment  $qx$  and causes an additional deflection  $x' = qx$  in the trajectories of all particles. It is convenient to describe this deflection in a phase space in which displacements and deflections are treated equally and independent of energy:  $\xi = x \cdot (\gamma\beta)^{1/2}$ ,  $\xi' = x' \cdot (\gamma\beta)^{1/2}$ , with  $\beta$  the local amplitude function; in this system coordinate pairs  $(\xi, \xi')$  for any particle fall on a circle with radius  $\epsilon^{1/2}$ , with  $\epsilon$  the invariant emittance of the particle, if the motion is linear. Using the previous expressions, we obtain for  $\xi'$  in terms of the emittance radius:

$$\left( \frac{\xi'}{\sqrt{\epsilon}} \right)_f = 2 \frac{\Delta x}{\rho} \left( \frac{1 + \text{sn}}{1 - \text{sn}} \right)^{1/2}, \quad \left( \frac{\xi'}{\sqrt{\epsilon}} \right)_d = 2 \frac{\Delta x}{\rho} \tag{A.2}$$

where  $\rho = l \cdot \text{sn} / (1 - \text{sn}^2)^{1/2}$  is the bending radius of the quadrupole.

The displacement of a quadrupole with inverse focal length  $q$  over a distance  $x$  from its reference position is equivalent to the introduction of a dipole moment  $qx$  and causes an additional deflection  $x' = qx$  in the trajectories of all particles. It is convenient to describe this deflection in a phase space in which displacements and deflections are treated equally and independent of energy:  $\xi = x \cdot (\gamma/\beta)^{1/2}$ ,  $\xi' = x' \cdot (\gamma\beta)^{1/2}$ , with  $\beta$  the local amplitude function; in this system coordinate pairs  $(\xi, \xi')$  for any particle fall on a circle with radius  $\varepsilon^{1/2}$ , with  $\varepsilon$  the invariant emittance of the particle, if the motion is linear. Using the previous expressions, we obtain for  $\xi'$  in terms of the emittance radius:

$$\left(\frac{\xi'}{\sqrt{\varepsilon}}\right)_f = 2 \frac{\Delta x}{\rho} \left(\frac{1 + \text{sn}}{1 - \text{sn}}\right)^{1/2}, \quad \left(\frac{\xi'}{\sqrt{\varepsilon}}\right)_d = 2 \frac{\Delta x}{\rho} \quad (\text{A.2})$$

where  $\rho = (\varepsilon\beta/g)^{1/2}$  is the (local) half beam width, with  $\varepsilon$  the emittance, and where subscripts  $f$  and  $d$  refer to focusing and defocusing quads. The errors  $\xi'$  appear at the exit of the linac rotated by their appropriate phase advances and contribute amounts  $\xi'_k \sin\psi_k$  and  $\xi'_k \cos\psi_k$  to the errors in position and direction at that point. The sum of all quadrupole misalignment errors is therefore:  $\Xi = \sum \xi'_k \sin\psi_k$ ,  $\Xi' = \sum \xi'_k \cos\psi_k$ . The  $\xi'_k$  are random variables, because their origins, the  $x_k$ , are so,  $\psi = k\Delta\psi/2$ , with  $k$  the number of half cells to the linac exit.

It may be seen, that for fixed  $x$ , the contribution to the error decreases with increasing beam half width  $\rho$  and with decreasing phase advance  $\Delta\psi$ . The maximum possible value for  $\rho$  is restricted to a small fraction of the operating wavelength of the linac by its physical structure, and is constant throughout its length. The available aperture is fully exploited if the beam width matches it everywhere. This can be done by keeping  $\beta/\gamma$  constant, thus, at constant  $\Delta\psi$ , by making the half cell length  $l$  proportional to the average energy in that cell.  $l$  will increase along the length of the linac in consequence, and the energy gain per cell with it. It follows that the total energy gain increases exponentially with the number of cells, this can be used to determine the number of half cells  $n$  in the machine:  $n = C \ln(\gamma_{\text{fin}}/\gamma_{\text{in}})$ , where  $C$  is a constant of integration, determined by the required focusing strength,  $\gamma_{\text{fin}}$  is the final energy and  $\gamma_{\text{in}}$  the injection energy. The value of  $C$  may be calculated as follows. The energy gain in the  $k^{\text{th}}$  half cell is:

2

$$\Delta E_k = (\gamma_k - \gamma_{k-1}) E_0 = \gamma_{k-1} E_0 (\exp(1/c) - 1) = l_k F_{tr} \bar{E}$$

where  $F_{tr} \bar{E}$  represents the net accelerating gradient. For  $l_k$  one may write:

$$l_k = \beta_{k-1} \text{sn} \sqrt{[(1 - \text{sn})/(1 + \text{sn})]} = \gamma_{k-1} \rho^2 \text{sn} \sqrt{[(1 - \text{sn})/(1 + \text{sn})]}/\epsilon,$$

if one assumes that the change in energy in a half cell may be disregarded in comparison with the average energy:  $(\gamma_{k-1} - \gamma_k) \ll (\gamma_{k-1} + \gamma_k)$ . This yields an expression for C:

$$C = 1/\ln \left( 1 + \frac{\rho^2}{\epsilon} \frac{F_{tr} \bar{E}}{E_0} \text{sn} \left( \frac{1 - \text{sn}}{1 + \text{sn}} \right)^{1/2} \right) \quad (\text{A.3a})$$

$$\approx \frac{\epsilon}{\rho^2} \frac{E_0}{F_{tr} \bar{E}} \frac{1}{\text{sn}} \left( \frac{1 + \text{sn}}{1 - \text{sn}} \right)^{1/2}, \text{ if } \frac{\rho^2}{\epsilon} \frac{F_{tr} \bar{E}}{E_0} \text{sn} \left( \frac{1 - \text{sn}}{1 + \text{sn}} \right)^{1/2} \ll 1 \quad (\text{A.3b})$$

The approximation appears to be acceptable for the cases under discussion here. With C available, the number of half cells, thus the number of quadrupoles, can be calculated and estimates of the error expectations due to quadrupole misalignments be made. Assuming that the errors  $x$  are uncorrelated and have equal rms values  $\Delta x_{\text{rms}}$ , we obtain:

$$\xi_{\text{rms}} = \left( \sum (\xi'_k \sin \psi_k)^2 \right)^{1/2} \quad \xi'_{\text{rms}} = \left( \sum (\xi'_k \sin \psi_k)^2 \right)^{1/2} \quad (\text{A.4})$$

This yields after some manipulation:

$$\frac{\xi_{\text{rms}}}{\sqrt{\epsilon}} = \frac{\xi'_{\text{rms}}}{\sqrt{\epsilon}} = 2 \frac{\Delta x_{\text{rms}}}{\rho} \left[ \frac{\epsilon}{\rho^2} \frac{E_0}{F_{tr} \bar{E}} \frac{1}{\text{sn}} \frac{(1 + \text{sn})^{1/2}}{(1 - \text{sn})^{3/2}} \ln \left( \frac{\gamma_{\text{fin}}}{\gamma_{\text{in}}} \right) \right]^{1/2} \quad (\text{A.5})$$

expectations due to quadrupole misalignments be made. Assuming that the errors  $x$  are uncorrelated and have equal rms values  $\Delta x_{\text{rms}}$ , we obtain:

$$\xi_{\text{rms}} = \left( \sum (\xi'_k \sin \psi_k)^2 \right)^{1/2} \quad \xi'_{\text{rms}} = \left( \sum (\xi'_k \sin \psi_k)^2 \right)^{1/2} \quad (\text{A.4})$$

This yields after some manipulation:

$$\frac{\xi_{\text{rms}}}{\sqrt{\epsilon}} = \frac{\xi'_{\text{rms}}}{\sqrt{\epsilon}} = 2 \frac{\Delta x_{\text{rms}}}{\rho} \left[ \frac{\epsilon}{\rho^2} \frac{E_0}{F_u \bar{E}} \frac{1}{\text{sn}} \frac{(1 + \text{sn})^{1/2}}{(1 - \text{sn})^{3/2}} \ln \left( \frac{\gamma_{\text{fin}}}{\gamma_{\text{in}}} \right) \right]^{1/2} \quad (\text{A.5})$$

This form can be minimized by choosing  $\text{sn} = (\sqrt{3}-1)/2 = 0.3660$ , i.e., by choosing the phase advance per cell  $\Delta\psi = 43^\circ$ ; the minimum is not very critical however, choosing  $\Delta\psi = 99^\circ$  instead of  $43^\circ$  increases  $\xi_{\text{rms}}$  with a factor 1.35. It is also evident that most of the damage is done at low energy, increasing the final energy by a factor 10 increases  $\xi_{\text{rms}}$  only with a factor 1.517. Substituting some numbers, we take  $\gamma_{\text{fin}}/\gamma_{\text{in}} = 10^4$ ,  $\text{sn} = 0.3660$ ,  $F_u \approx 2/3$ ,  $\bar{E} = 10^9 \text{V/m}$  and  $\rho = 0.02\lambda$  and obtain:

$$\frac{\xi_{\text{rms}}}{\sqrt{\epsilon}} = \frac{\xi'_{\text{rms}}}{\sqrt{\epsilon}} \approx 1000 \frac{\Delta x_{\text{rms}}}{\lambda^2} \sqrt{\epsilon} \quad (\text{A.6})$$

The displacement of the beam axis as a fraction of the half beam width and its directional deviation as a fraction of the half angular spread are both equal to  $\xi/\sqrt{\epsilon}$ . It may be seen from (5.2.1), that, crudely speaking,  $\epsilon/\lambda^2$  is constant; for the conditions shown:  $\epsilon/\lambda^2 \approx 1$ . Using this we find

$$\frac{\xi_{\text{rms}}}{\sqrt{\epsilon}} = \frac{\xi'_{\text{rms}}}{\sqrt{\epsilon}} \approx 1000 \frac{\Delta x_{\text{rms}}}{\lambda} \approx 39 \Delta x_{\text{rms}} B^{0.34} \quad (\text{A.7})$$

where  $B$  is the brightness of the beam, as defined earlier. For a jitter in the coordinates of the axis of  $\xi_{rms}/\sqrt{\epsilon} \leq 0.1$ ,  $\Delta\xi_{rms} \leq 0.0026B^{0.34}$  has to be realized, thus  $\Delta\xi_{rms} \leq 1 \mu\text{m}$  at  $B = 10^{10} \text{A}/(\text{rad}\cdot\text{m})^2$ , and  $\Delta\xi_{rms} = 9 \text{nm}$  at  $B = 10^{16} \text{A}/(\text{rad}\cdot\text{m})^2$ .

A linac could also be focused by linac sections as described in Section 5.2. A similar calculation for that case yields:

$$\text{sn} = \sin(\Delta\psi) = 0.5\sqrt{l/q} \quad (\text{A.8})$$

$$\beta = \frac{l}{2\text{sn}(1 - \text{sn}^2)^{1/2}} \quad (\text{A.9})$$

$$C = 1/\ln \left( 1 + 2\text{sn}(1 - \text{sn}^2)^{1/2} \frac{\rho^2 F_{ur} \bar{E}}{\epsilon E_o} \right) \approx \frac{\epsilon E_o}{2\rho^2 F_{ur} \bar{E}} \frac{1}{\text{sn}(1 - \text{sn}^2)^{1/2}} \quad (\text{A.10})$$

$$n \approx \frac{\epsilon E_o}{2\rho^2 F_{ur} \bar{E}} \frac{1}{\text{sn}(1 - \text{sn}^2)^{1/2}} \ln \left( \frac{\gamma_{fin}}{\gamma_{in}} \right) \quad (\text{A.11})$$

$$\frac{\zeta_{rms}}{\sqrt{\epsilon}} = \frac{\zeta'_{rms}}{\sqrt{\epsilon}} = \frac{\Delta x_{rms}}{\rho} \left[ \frac{\epsilon E_o}{\rho^2 F_{ur} \bar{E}} \frac{\text{sn}}{(1 - \text{sn}^2)^{3/2}} \ln \left( \frac{\gamma_{fin}}{\gamma_{in}} \right) \right]^{1/2} \quad (\text{A.12})$$

Now it seems best to choose  $\text{sn}$ , thus the phase advance per cell small. It cannot be chosen arbitrarily small however, because  $\beta$  must have a predetermined value:  $\beta = \rho^2 \epsilon / \gamma$ ; we do not develop this subject any further here. Another matter is, that the choice of a fixed phase advance per cell combined with a variable cell length, was arbitrary: a fixed cell length and a variable phase advance seems equally possible and may be advantageous.

FINAL FOCUS

Consider a final focusing system with transfer matrix (for the x coordinate):  $|M| = \begin{vmatrix} 0 & R \\ -1/R & 0 \end{vmatrix}$  relative to its axis. The system may consist of several lenses and drift spaces, but is regarded as a single, rigid device, that may be transversely misaligned relative to some external reference system. Its axis is straight, and the distance between entrance and exit planes, measured along that axis, is D. Let this system axis be misaligned by  $\xi_{en}$  and  $\xi'_{en}$ , relative to the reference, in the entrance plane. Its coordinates  $(\xi, \xi')_{ex}$  in the exit plane are then:  $\begin{vmatrix} \xi \\ \xi' \end{vmatrix}_{ex} = \begin{vmatrix} 1 & D \\ 0 & 1 \end{vmatrix} \begin{vmatrix} \xi \\ \xi' \end{vmatrix}_{en}$ . The coordinates  $(x, x')_{en}$  of a sample particle, relative to the reference at the system entrance, are transformed to  $(x, x')_{ex}$  at its exit according to:

$$\begin{vmatrix} x \\ x' \end{vmatrix}_{ex} = \begin{vmatrix} 0 & R \\ -1/R & 0 \end{vmatrix} \begin{vmatrix} x \\ x' \end{vmatrix}_{en} + \begin{vmatrix} 1 & D-R \\ -1/R & 1 \end{vmatrix} \begin{vmatrix} \xi \\ \xi' \end{vmatrix}_{en} \quad (B.1)$$

It follows that the misalignment changes the coordinates of the beam axis by

$$\begin{vmatrix} xa \\ xa' \end{vmatrix}_{ex} = \begin{vmatrix} 1 & D-R \\ -1/R & 1 \end{vmatrix} \begin{vmatrix} \xi \\ \xi' \end{vmatrix}_{en} \quad (B.2)$$

at the exit of the system. It is evident that the axis moves as much as the system does in cases of system translation ( $\xi' = 0$ ), and that it is rotated in addition.

There are two, presumably identical, such final foci in a linear collider, one for each beam. Each of them affects its associated beam in the manner described above, although it has to be kept in mind, that transverse displacements are counted positive in opposite directions for beams that move in opposite directions. The changes in distance  $\delta x$  and angle  $\delta x'$  between the two beams in response to changes in the coordinates of the final foci are therefore:

$$\begin{vmatrix} \delta x \\ \delta x' \end{vmatrix} = \begin{vmatrix} xa_1 + xa_r \\ xa_1 - xa_r \end{vmatrix}_{ex} = \begin{vmatrix} 1 & D-R \\ -1/R & 1 \end{vmatrix} \begin{vmatrix} \xi_1 + \xi_r \\ \xi_1 - \xi_r \end{vmatrix}_{en} \quad (B.3)$$

where subscripts  $_l$  and  $_r$  label the left hand and right hand sides of the crossing point. The misalignments  $(\xi, \xi')_{en}$  are likely to be uncorrelated random variables if the two final foci are physically separate units and the standard deviations of the differences in the coordinates of the beamaxes  $\delta x$ ,  $\delta x'$ ,  $\delta y$  and  $\delta y'$  will be controlled by the standard deviations in the misalignments:  $\xi_1 \sqrt{2}$ ,  $\xi_r \sqrt{2}$ ,  $\eta_1 \sqrt{2}$  and  $\eta_r \sqrt{2}$ . This changes if they can be integrated into a single physical unit. Expressing  $\xi_{l,r}$  and  $\xi'_{l,r}$  as translations and rotations  $\xi$  and  $\xi'$  of that combined unit we obtain:

$$\begin{aligned}
 \xi_l &= \xi + D\xi' \\
 \xi_r &= -\xi + D\xi' \\
 \xi_l' &= \xi_r' = \xi'
 \end{aligned}
 \tag{B.4}$$

In terms of these new variables the relative misalignment of the beamaxes becomes:

$$\begin{vmatrix} \delta x \\ \delta x' \end{vmatrix} = \begin{vmatrix} 1 & D-R \\ -1/R & 1 \end{vmatrix} \begin{vmatrix} D\xi' \\ 0 \end{vmatrix}$$
(B.5)

It may be seen, that the beam misalignment is primarily affected by rotations of the final focusing system, and that it is important to keep it short, i.e., D small, to minimize the sensitivity to such rotations.

A similar calculation for a final focus with a transfer matrix of the form  $|M| = \begin{vmatrix} -A & 0 \\ 0 & 1/A \end{vmatrix}$  yielded:

$$\begin{vmatrix} \delta x \\ \delta x' \end{vmatrix} = \begin{vmatrix} xa_l + xa_r \\ xa_l' + xa_r' \end{vmatrix}_{ex} = \begin{vmatrix} 1+A & D \\ 0 & 1+1/A \end{vmatrix} \begin{vmatrix} \xi_l + \xi_r \\ \xi_l' - \xi_r' \end{vmatrix}_{en} = \begin{vmatrix} 1+A & D \\ 0 & 1+1/A \end{vmatrix} \begin{vmatrix} D\xi' \\ 0 \end{vmatrix}$$
(B.6)

In cases of practical interest  $A \ll 1$ , so that:

$$\begin{vmatrix} \delta x \\ \delta x' \end{vmatrix} = \begin{vmatrix} 1 & D \\ 0 & 1/A \end{vmatrix} \begin{vmatrix} D\xi' \\ 0 \end{vmatrix}$$
(B.7)

which emphasizes again the importance of keeping the length D and the angular misalignment  $\xi'$  small.



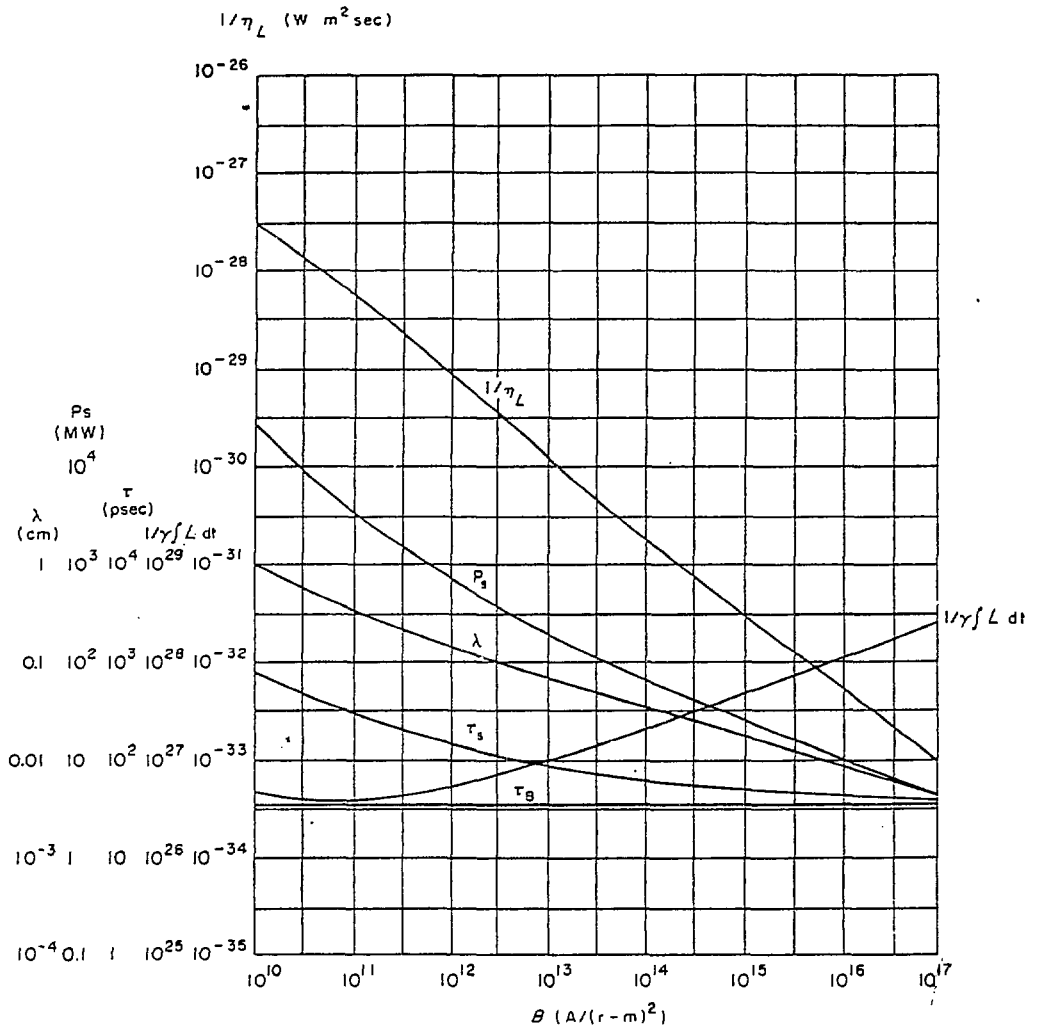


Fig. 4.1  $1/\eta_L$ ,  $\frac{1}{\gamma}Ldt$ ,  $\lambda$ ,  $P_s$ ,  $\tau_s$  and  $\tau_B$  as functions of  $B$  for optimized values of  $\lambda$  and  $R_0$ .

$$\bar{E} = 10^9 V/m, L_B = 1cm, \bar{\alpha} = 0.05$$

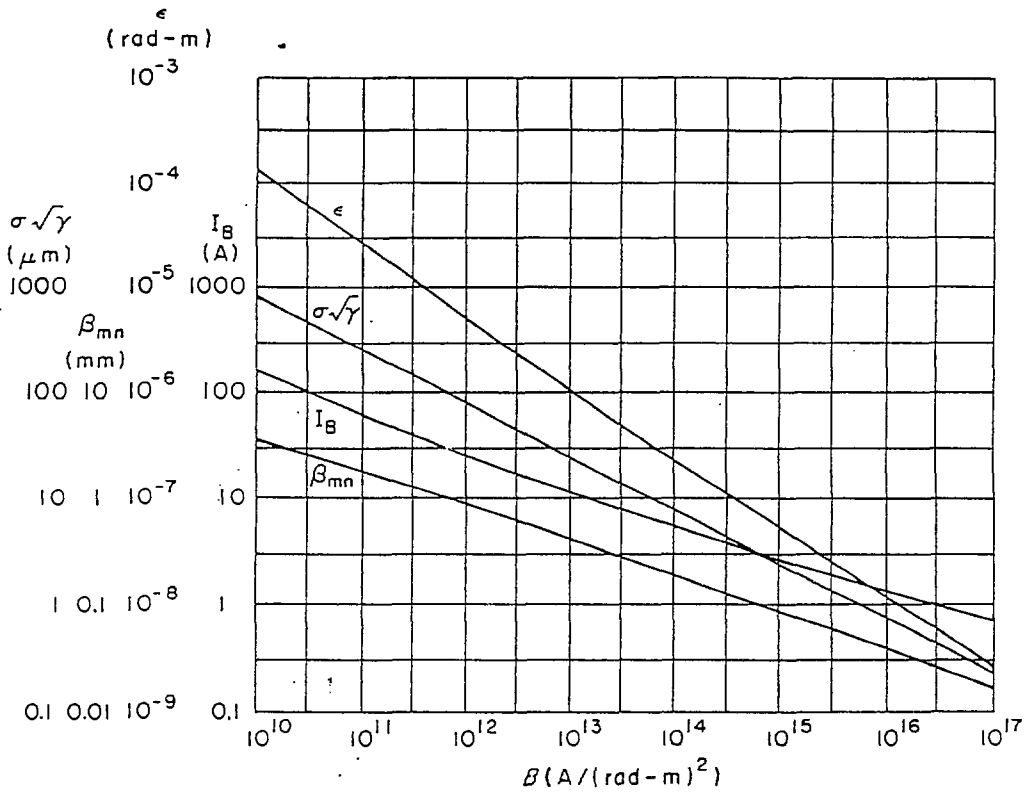


Fig. 4.2  $\epsilon$ ,  $\sigma\sqrt{\gamma}$ ,  $I_B$  and  $\beta_{mn}$  as functions of  $B$  for optimized values of  $\lambda$  and  $R_0$ .

$$\bar{E} = 10^9 \text{V/m}, L_B = 1 \text{cm}, \bar{\alpha} = 0.05$$

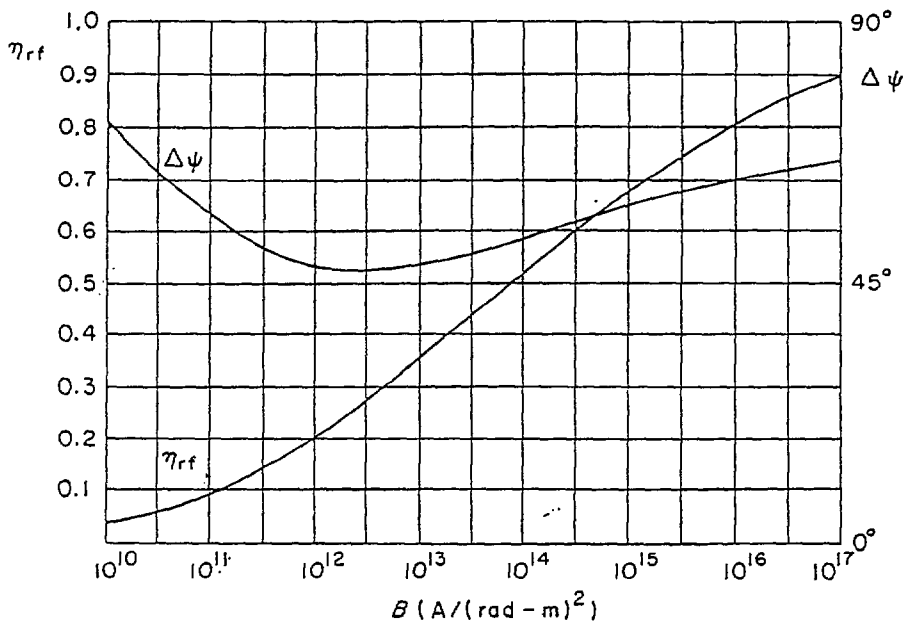


Fig. 4.3  $\Delta\psi$  and  $\eta_{rf}$  as functions of  $B$  for optimized values of  $\lambda$  and  $R_{o_i}$

$$E = 10^9 \text{ V/m}, L_B = 1 \text{ cm}, \bar{\alpha} = 0.05$$

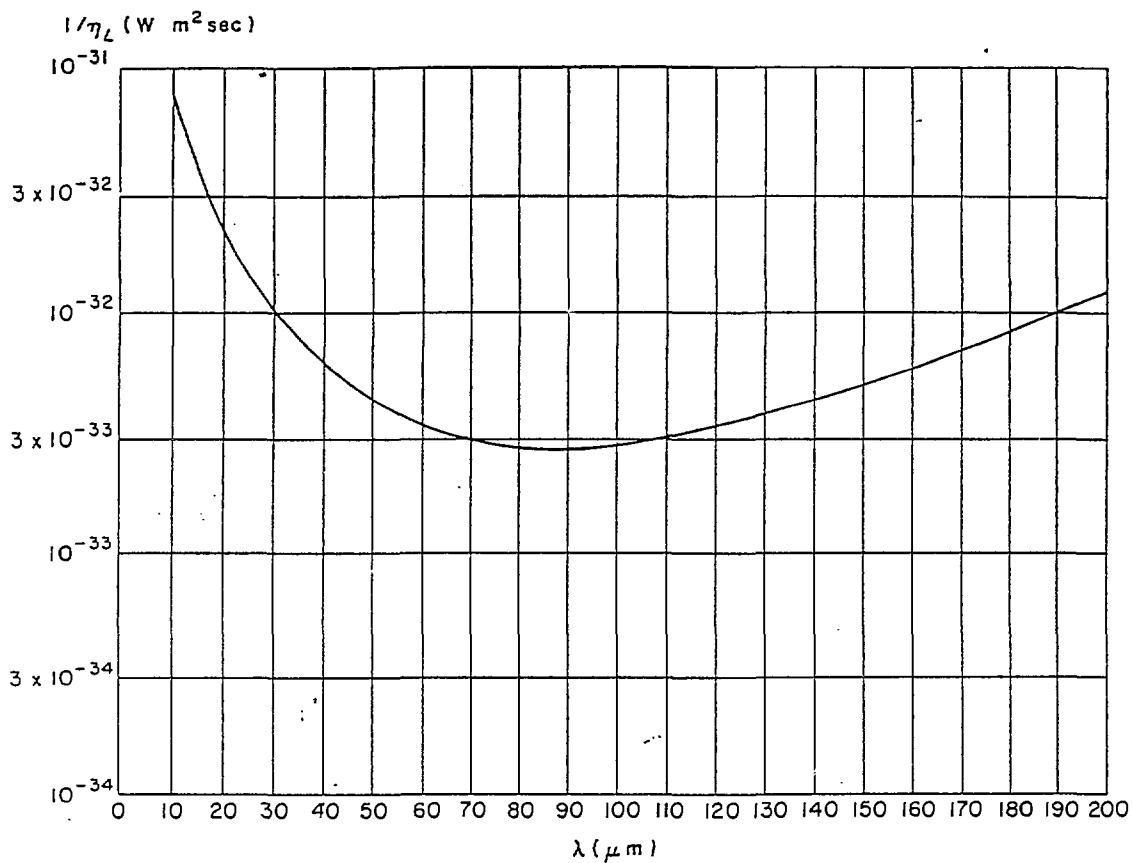


Fig. 4.4  $1/\eta_L = f(\lambda)$  for  $B = 10^{16} \text{ A}/(\text{rad}\cdot\text{m})^2$ ,  $R_0$  optimized.

$$\bar{E} = 10^9 \text{ V/m}, L_B = 1 \text{ cm}, \bar{\alpha} = 0.05$$

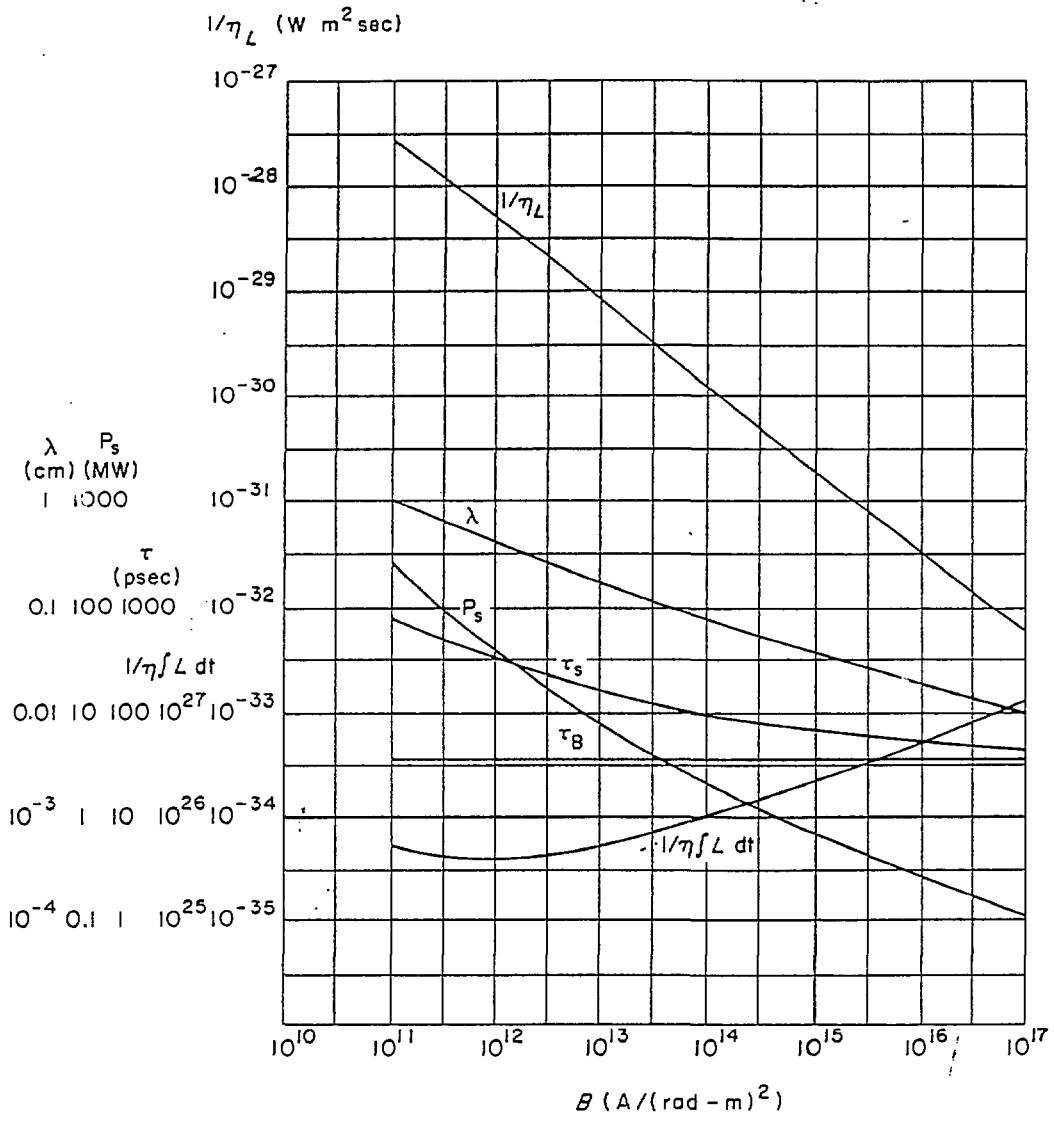


Fig. 4.5  $1/\eta_L$ ,  $\frac{1}{\lambda} \int L dt$ ,  $\lambda$ ,  $P_s$ ,  $\tau_s$  and  $\tau_B$  as functions of  $B$  for optimized values of  $\lambda$  and  $R_0$ .  
 $E = 10^8$  V/m,  $L_B = 1$  cm,  $\bar{\alpha} = 0.05$

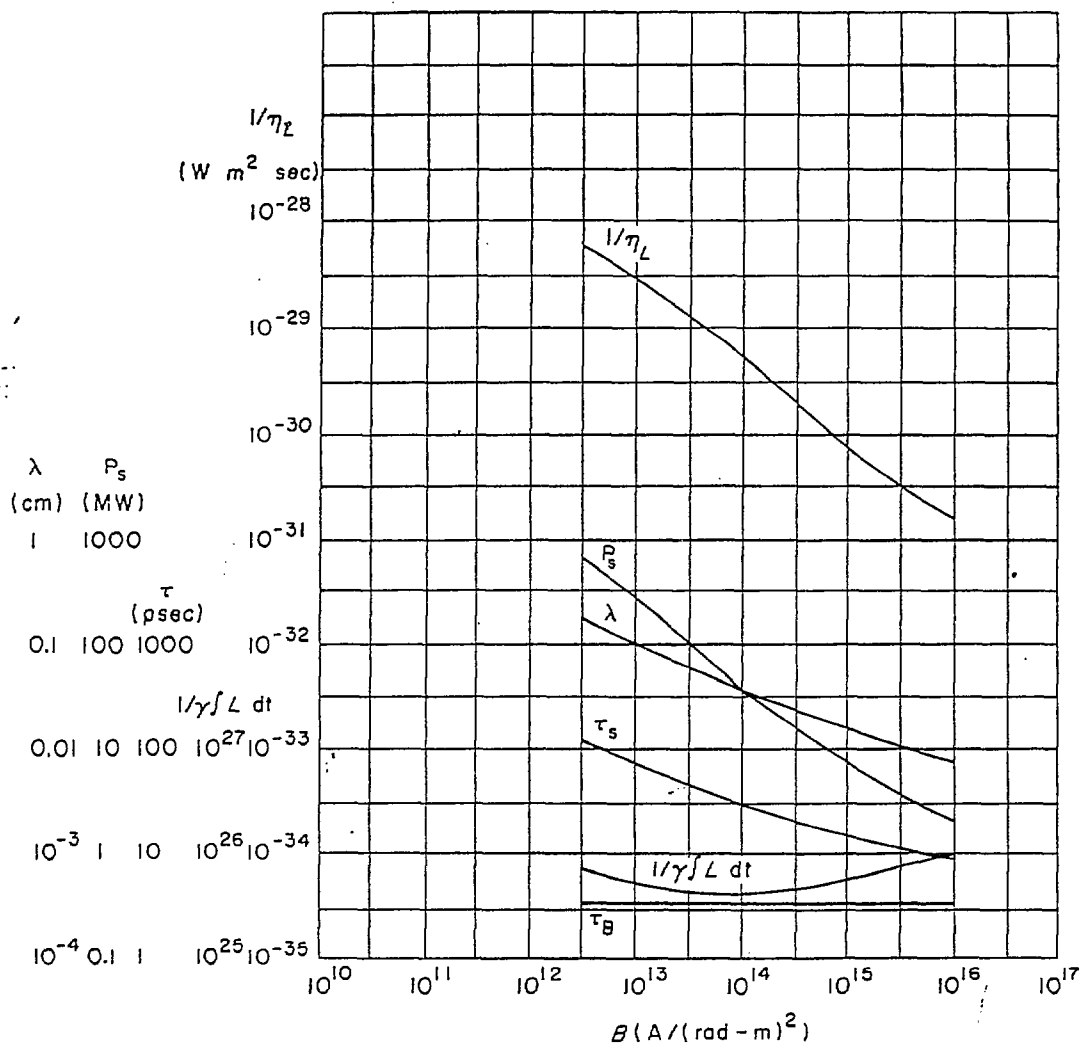


Fig. 4.6  $1/\eta_L$ ,  $\frac{1}{\lambda} \int L dt$ ,  $\lambda$ ,  $P_s$ ,  $\tau_s$  and  $\tau_B$  as functions of  $B$  for optimized values of  $\lambda$  and  $R_0$ .

$$E = 10^9 V/m, L_B = 0.1 cm, \bar{\alpha} = 0.05$$

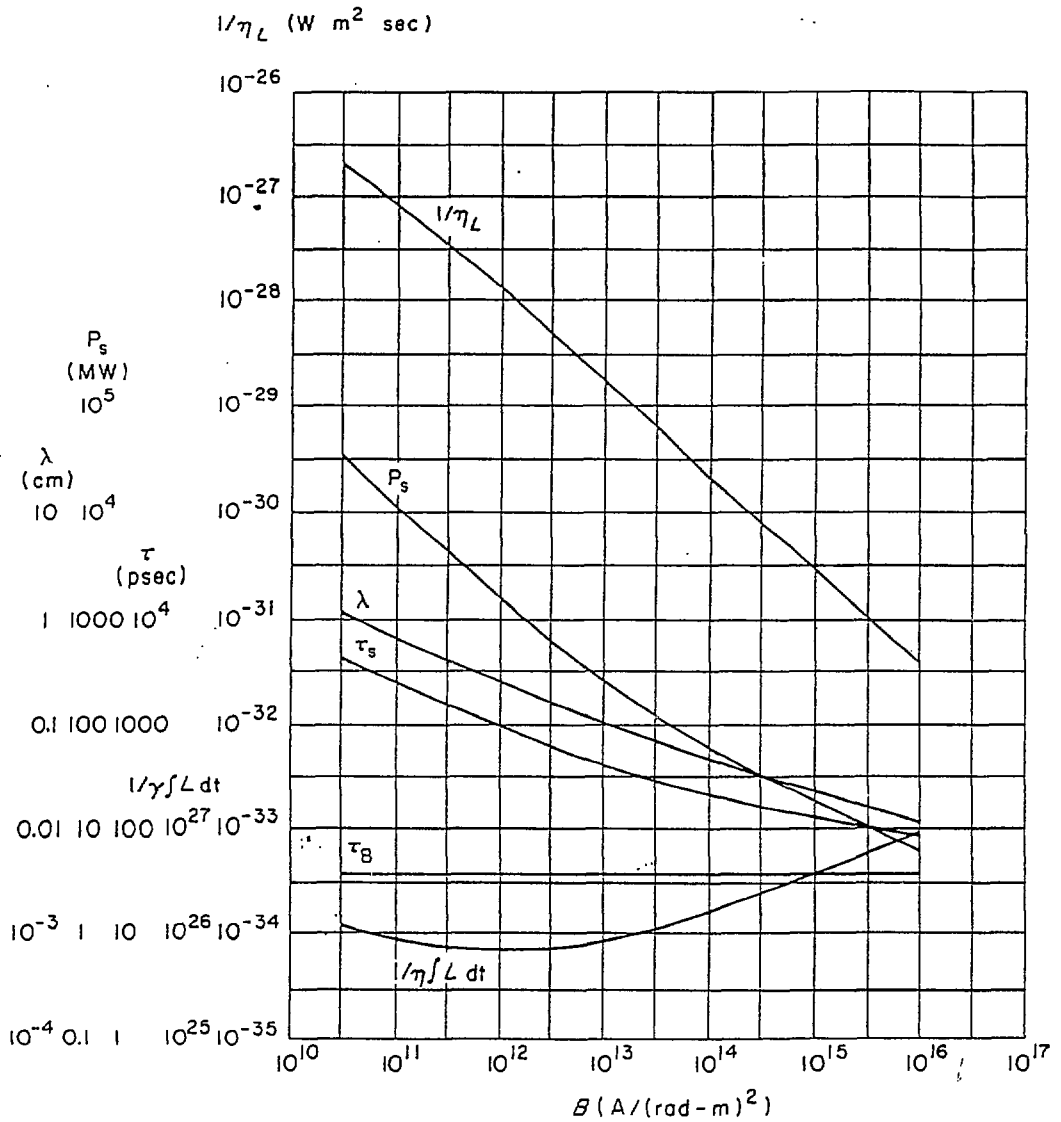


Fig. 4.7  $1/\eta_L$ ,  $\frac{1}{\lambda} \int L dt$ ,  $\lambda$ ,  $P_s$ ,  $\tau_s$  and  $\tau_B$  as functions of  $B$  for optimized values of  $\lambda$  and  $R_0$ .

$$E = 10^9 V/m, L_B = 1 \text{ cm}, \bar{\alpha} = 0.01$$

## **DISCLAIMER**

This report was prepared as an account of work sponsored by an agency of the United States Government. Neither the United States Government nor any agency thereof, nor any of their employees, makes any warranty, express or implied, or assumes any legal liability or responsibility for the accuracy, completeness, or usefulness of any information, apparatus, product, or process disclosed, or represents that its use would not infringe privately owned rights. Reference herein to any specific commercial product, process, or service by trade name, trademark, manufacturer, or otherwise does not necessarily constitute or imply its endorsement, recommendation, or favoring by the United States Government or any agency thereof. The views and opinions of authors expressed herein do not necessarily state or reflect those of the United States Government or any agency thereof.